THE ASTROPHYSICAL JOURNAL, 382:652–666, 1991 December 1

SIGNATURES OF COSMIC-RAY INTERACTIONS ON THE SOLAR SURFACE

D. SECKEL, TODOR STANEV, AND T. K. GAISSER
Bartol Research Institute, University of Delaware, Newark, DE 19716
Received 1991 March 21; accepted 1991 June 5

ABSTRACT

We estimate the fluxes of neutrinos, gamma rays, antiprotons, neutrons, and antineutrons that result from collisions of high-energy Galactic cosmic rays with the solar atmosphere. The results are sensitive to assumptions about cosmic-ray transport in the magnetic fields of the inner solar system. The high-energy photon flux should be observable by the Gamma Ray Observatory. The neutrino flux should produce less than one event per year in the next generation of neutrino telescopes. The antiproton flux is unobservable against the Galactic background. The neutron and antineutron fluxes are detectable only if neutrons produced in terrestrial cosmic-ray events may be discriminated against.

Subject headings: cosmic rays: general — gamma rays: general — neutrinos — Sun: activity

1. INTRODUCTION

The interactions of high-energy cosmic-ray nuclei with matter have been studied in a variety of settings. In our own atmosphere, these interactions produce cascades which include, or in turn produce, detectable fluxes of electrons, positrons, muons, gamma rays, Čerenkov light, neutrons and other nuclear fragments, and neutrinos. Interactions with interstellar gas are thought to produce the observed Galactic flux of γ-rays (Mayer-Hasselwander et al. 1982; Fichtel & Kniffen 1984; Fichtel et al. 1977) with energies above $\sim$500 MeV, antiprotons (Stephens & Golden 1987), and positrons (Protheroe 1982). In this paper we explore another place where interactions between cosmic-ray nuclei and gas may produce observable signals: the Sun.

At first, the Sun may seem an inappropriate source. Although nearby, it covers a fairly small fraction of the sky: $(\pi R_\odot^2/4\pi r_\oplus^2) = 5.5 \times 10^{-6}$, where $R_\odot = 7.0 \times 10^{10}$ cm and $r_\oplus = 1$ AU $= 1.5 \times 10^{13}$ cm. Therefore, if the same flux of cosmic rays impinged on the Sun as on the Earth, the total flux of byproducts from the Sun would be much suppressed. However, if one can resolve the source, then surface brightness is the relevant criterion for detection and, neglecting details of cosmic-ray absorption by the Sun (magnetic fields, composition and density of the Sun, etc.), one expects comparable surface brightness for the terrestrial and solar sources. For neutrinos, which can only be detected at Earth, the signal from the Sun should therefore be at least equal to the atmospheric background. The other signals (γ-rays, neutrons) must be observed from space, with a low background due to cosmic-ray interactions with intergalactic gas. Thus, as long as the Sun can be resolved, the flux of byproducts from solar cascades should not be background limited.

Unfortunately, a number of messy details have been passed over which cannot be ignored. First, one may expect the flux of cosmic rays absorbed by the Sun to be reduced from that incident upon the Earth due to the magnetic fields in the inner solar system. The interplanetary magnetic field (IMF), coronal fields, and photospheric fields may all play a role in generating "heliomagnetic" effects.

Second, geometric effects, such as shadowing, must be considered. If one were to look back at Earth for similar signals, then only the skin of Earth's atmosphere would have the appropriate thickness to generate high-energy photons without reabsorbing them. The high-energy cascade products would then be suppressed from the naive value by an amount of order $h_\oplus/R_\oplus \sim 10^{-3}$, where $h_\oplus$ is the scale height of Earth's atmosphere, and $R_\oplus$ is Earth's radius. Although we will argue otherwise, one might worry that a similar suppression occurs for the Sun.

Third, to calculate fluxes from the Sun, one must take into account the details of the solar atmosphere. For example, typical cascades will take place in a less dense environment than for Earth, and that increases the yields of some by-products.

Despite these uncertainties, it is possible to make some quick estimates of the fluxes of by-products. The total cosmic-ray flux of nucleons above 1 GeV is $I_{cr}(E > 1 \text{ GeV}) \simeq 1 \text{ cm}^{-2} \text{ s}^{-1} \text{ sr}^{-1}$. Absorbing this primary flux on the solar disk and reemitting the byproducts isotropically would generate a secondary flux of $\sim 10^{-4} \text{ cm}^{-2} \text{ s}^{-1}$. Including a factor of, say, 10^{-3} suppression due to heliomagnetic effects, absorption of byproducts by the Sun, etc., would give a flux of order $10^{-7} \text{ cm}^{-2} \text{ s}^{-1}$ of high-energy cascade products. Such a flux of photons should be detectable by the EGRET instrument of the Gamma Ray Observatory (GRO) (Kanbach et al. 1989). For neutrinos, a similar argument includes just higher energy cosmic rays (say above 100 GeV) and the suppressions compared to Earth should not be so severe. Taking $10^{-8} \text{ cm}^{-2} \text{ s}^{-1}$ as an estimate of the integrated flux above 100 GeV gives a signal which just misses being detectable in currently planned neutrino telescopes (Baldo Ceolin 1990).

The previous paragraph gives us the first motivation for this work: current technology is improving to the point that cosmic-ray interactions in the Sun may soon be detectable. This is certainly true for the case of GeV γ-rays, which may be observed by GRO.

We have argued that an interstellar flux of protons incident on the solar surface would be observable in γ-rays, but that it is likely that an interstellar flux is inappropriate due to the presence of magnetic fields in the inner solar system. Therefore, a second motivation for this work is that observations of cosmic-ray interactions on the solar surface will give us indirect information about the propagation of charged particles in the inner solar system. In this regard, we note that many aspects of our

problem are similar to those confronted in trying to understand solar flares (Murphy, Dermer, & Ramaty 1987; Ramaty et al. 1990).

A third motivation concerns the detectability of dark matter (Primack, Seckel, & Sadoulet 1988). Current wisdom holds that ~90% of our galaxy consists of a form of matter which is still to be identified. A class of particle candidates known as WIMPs (weakly interacting massive particles) may be captured by the Sun in significant numbers. Once captured, they may annihilate with each other, sometimes producing ~GeV neutrinos in the annihilation products (Silk, Olive, & Srednicki 1985; Gelmini, Gondolo, & Roulet 1991; Kamionkowski 1990). Neutrino data from all the large proton decay experiments has been analyzed to search for this signal; so far these searches have been negative (Sato et al. 1990; Losecco et al. 1987; Casper 1990; Kuznik 1987). One purpose of the present work is to evaluate whether cosmic-ray interactions on the solar surface will eventually constitute an important background to future searches for dark matter–produced neutrinos.

Finally, a current problem in cosmic-ray physics is that the antiproton-to-proton ratio in the interstellar cosmic-ray flux is higher than can be explained by the simplest models (Stephens & Golden 1987; Gaisser & Schaefer 1991). One may wonder if that flux may be produced locally. We will argue that the local flux of solar-produced $\bar{p}$'s is at least two orders of magnitude lower than observations and cannot explain the surplus.

The issues raised above suggest that it is time for a serious calculation of these processes. As a starting point, in § 2 we give a phenomenological description of the stellar atmosphere, stellar magnetic fields, and the interplanetary magnetic fields. With this input as justification, we develop a model for the absorption of cosmic rays by the Sun, including effects due to the interplanetary and solar magnetic fields. The model also determines where in the Sun interactions take place and, therefore, how the local environment will affect shower development. In the succeeding sections, we use that model as the basis for Monte Carlo calculations of the flux of neutrinos, γ-rays, antiprotons, and neutrons from cosmic-ray interactions in the Sun. For each product, we discuss the experimental issues associated with the detection of our predicted fluxes. We summarize our conclusions in § 6.

Finally, a note on terminology. We were tempted to use the term "albedo" to describe the flux of cascade products emanating from the Sun; however, that word carries a connotation of flux reflected from a surface, which is not appropriate for all the signals we discuss. Specifically, most of the observable flux of neutrinos is actually produced on the back side of the Sun and passes through the Sun on the way to Earth. The flux of photons and neutrons, however, does come from the terrestrial side of the Sun, and there the use of "albedo" makes sense. We therefore refer to our signals generically as a flux of high-energy cascade products, but when discussing the photon and neutron fluxes we often use the word "albedo."

2. COSMIC-RAY ABSORPTION BY THE SUN

In order to calculate the fluxes of neutrinos, photons, and baryons produced by cosmic-ray interactions with the Sun we must have a model for how these interactions take place. Our model involves two steps: propagating the cosmic-ray protons to the interaction region, and determining the local nature of the interactions and the resultant showers. As input to our model, we first describe the structure of the solar atmosphere and the magnetic fields in the inner solar system. We then proceed to the questions of propagation and a detailed description of the showers.

2.1. *Structure of the Solar Atmosphere and Magnetic Fields in the Inner Solar System*

The structure of the solar atmosphere is complex. Above the photosphere, there is a temperature minimum in the lower chromosphere of about 4000 K above which the temperature rises slowly until there is an abrupt transition to a $\sim 10^6$ K corona. This transition occurs about 1000 km above the photosphere depending in detail upon the local conditions. For our purposes it is sufficient to describe the chromosphere as an isothermal atmosphere in hydrostatic equilibrium:

$$\rho = \rho_0 e^{-z/h} ,$$
$$h = \frac{kTR_\odot^2}{\mu G_N M_\odot} \simeq 115 \text{ km} , \qquad (2.1)$$
$$\rho_0 \simeq 4 \times 10^{-7} \text{ g cm}^{-3} ,$$

where z is the height above the photosphere, h is an average scale height in the chromosphere, ρ_0 is the density at the photosphere, k is Boltzmann's constant, G_N is Newton's constant, $M_\odot$ is a solar mass, and μ is the mean molecular weight of the gas. The value of $h = 115$ km is taken from Figure 7 of Vernazza, Avrett, & Loeser (1973). The density at the bottom of the corona is of order 10^{10} cm^{-3}. For matter in the corona a simple scale-height description is inappropriate; however, the density is so low that little absorption of cosmic-ray flux takes place in the corona, and we do not need a good model of coronal densities.

Just below the photosphere the atmosphere becomes convective, with adiabatic exponents that vary with the ionization state of the gas. In Figure 1 we show the density and column density, $x(z) = \int^z \rho(z')dz'$ as a function of depth below the photosphere (Baker & Temesvary 1966). The column density includes a contribution, $h\rho_0 \simeq 4$ g cm^{-2}, due to integrating above the photosphere. Relevant depths will be: x(500

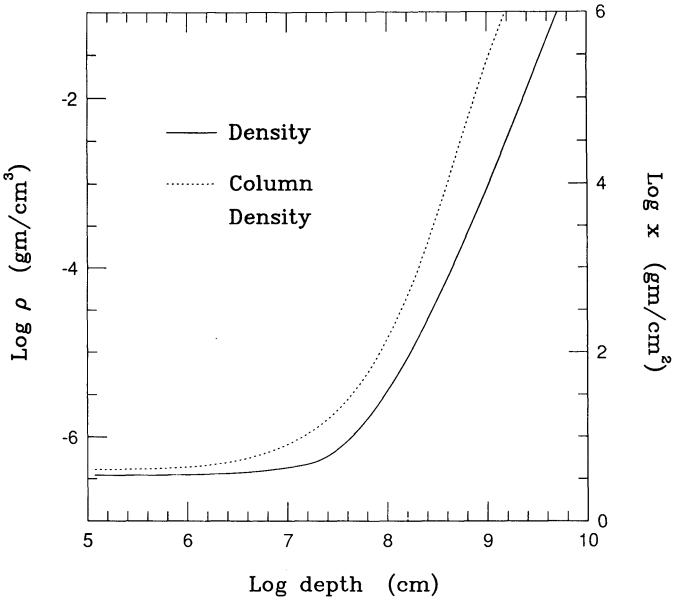

FIG. 1.—Density and column density as a function of depth below the photosphere, from Baker & Temesvary (1966).

km) ≈ 40 g cm^{-2}, where the incoming cosmic-ray flux has suffered one absorption length; $x(900 \text{ km}) \approx 100$ g cm^{-2}, where pions get absorbed; and $x(10{,}000 \text{ km}) \approx 10^5$–$10^6$ g cm^{-2}, where muons with $E \gtrsim 1$ TeV will stop.

We must also discuss the model for magnetic fields that we use. We divide space into three regions: interplanetary space, the corona, and the regions below the corona. For $r > 2R_\odot$, the average interplanetary magnetic field (IMF) is given by Parker (1958) as

$$B_r = \frac{a}{r^2}\Theta\,,$$
$$B_\theta = 0\,, \qquad (2.2)$$
$$B_\phi = -\frac{b}{r}\Theta\,,$$

where $\Theta = \pm 1$ in the northern/southern hemisphere. Typical field strength at Earth is $B_\oplus \sim 5 \times 10^{-5}$ G, with a spiral angle of order 45°. Interior to Earth's orbit the field is nearly radial. In addition to the average field, there are fluctuations in the field strength that presumably act to scatter charged particles. We deal with these fluctuations by treating the propagation of charged particles in the IMF as a diffusion problem.

In the chromosphere and below the photosphere, we will assume a magnetic field configuration appropriate for a "quiet" Sun (Priest 1982). The important features of this model are illustrated in Figure 2. Average field strengths are on the order of a few gauss, but the fields are not homogenous. Most of the flux is carried by flux bundles which have field strengths of $\sim 10^3$ G and horizontal dimensions on the order of a few hundred kilometers. The bundles are located at the corners of convective cells and so are separated by thousands of kilometers. Thus, the bundles occupy a small fraction of the surface area, with the interbundle regions assumed to be nearly field free. Above the surface, the bundles are thought to broaden and diminish, maintaining approximate equilibrium between gas pressure and magnetic pressure. Above the chromosphere-corona transition the magnetic pressure dominates, and the magnetic fields form a "canopy" with average fields strengths of order of a few gauss.

The field strengths in the corona are not well known: "*Since it is so difficult to measure coronal magnetic fields, solar astronomers have resorted to calculating them,*" (Zirker 1981). We will assume that the field strengths in the upper corona diminish to ~ 1 G, eventually matching onto the IMF. We note that for certain regions of the Sun—for example, "active regions" and sunspots—the field strengths are considerably stronger. Although these regions may be of most interest to solar physicists and are the best studied, we do not feel that they represent the magnetic fields appropriate for describing the mean propagation of cosmic-ray protons in the solar atmosphere.

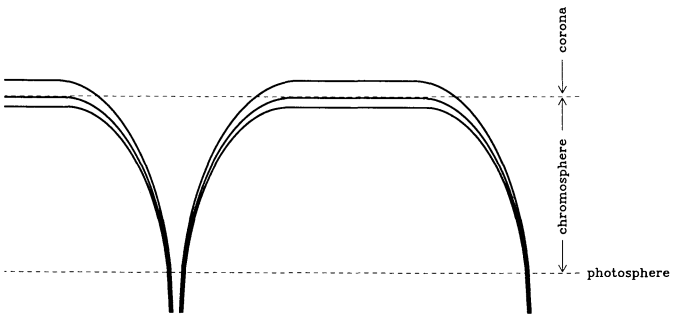

FIG. 2.—Schematic representation of solar magnetic fields near the photosphere.

Any cosmic-ray protons that are to interact with the solar atmosphere must somehow propagate from interplanetary space through the corona, chromosphere, and photosphere down to a depth of ~ 500 km where they are absorbed. By analogy with Earth's fields one might expect a severe heliomagnetic cutoff at an energy where the gyroradius of incident particles becomes less than the radial extent of the magnetic fields. For the Sun this would imply a cutoff at about 10^4 GeV. There is, however, an important difference between Earth and the Sun. Near Earth most IMF field lines are shunted around Earth by Earth's own dipole field. Only a small fraction of IMF field lines come down to the surface at Earth's poles. The Sun, however, is the source of the interplanetary magnetic field, and nearly all IMF field lines eventually end on the solar surface. Therefore, it is appropriate to note that in the polar regions the field is fairly homogenous with most field lines open to the IMF. In the midlatitude and equatorial regions most coronal field lines end back on the photosphere, although a nonzero fraction are still open through "coronal holes." The fraction of IMF lines that end in polar regions varies with time, increasing during solar maximum and decreasing at solar minimum (Zirker 1981).

2.2. *Cosmic-Ray Absorption by the Sun*

The complicated phenomenology of the inner solar system precludes a complete description of charged particle propagation in the inner solar system. It is, therefore, appropriate to construct simple models which should (1) make some phenomenological sense and (2) have the flexibility to test the sensitivity of our results to plausible assumptions about particle transport.

Our models have two parts: the inner solar system from Earth orbit down to the bottom of the corona is treated as a diffusion problem with no absorption. In order to solve the diffusion problem it is necessary to impose a boundary condition at the bottom of the corona, which takes the form of absorption and reflection coefficients.

Interior to the corona, we treat absorption and propagation simultaneously. We follow classical particle orbits in a fixed magnetic field configuration, which should be acceptable for relativistic cosmic rays making short excursions into the surface magnetic flux tubes. We use the interior model to estimate the overall absorption and reflection coefficients for the inner boundary condition to the diffusion problem. It also supplies a detailed model for where cosmic rays interact in the solar atmosphere and gives the distribution of zenith angles for the primaries when they interact. This information is needed in calculating the probability that photons or neutrons will escape the Sun to be seen at Earth.

We should, perhaps, justify our different treatments of propagation interior to, within, and outside the corona. We feel that cosmic-ray studies supply enough data to constrain a diffusion model for the IMF. Near the solar surface we have no direct handle on propagation, but sufficient data exists about magnetic fields in the photosphere to construct a direct model of particle orbits. Continuing the diffusive treatment of the IMF into the corona is done as a matter of convenience, but

there is no reason to suspect that this leads to gross errors in our predictions. We discuss the relevant quantities in § 2.2.2.

Before describing the more involved model it is useful to consider a naive estimate for the incident flux, ignoring any effects due to solar magnetic fields or the IMF. In this model, the solar surface is taken to be fully absorbing, and zenith angles are determined solely by geometric considerations. Since the effect of magnetic fields is to reduce the rate at which cosmic rays interact with the Sun, this model places an upper bound on the signals we consider.

The total absorption rate of cosmic rays is given by

$$\Gamma(E) = 4\pi r^2 j(E) , \tag{2.3}$$

where j is the *net* differential flux (i.e., $j = 0$ for an isotropic velocity distribution) of cosmic rays. In the simple model which ignores magnetic fields, j is given by

$$j_N = \frac{1}{4}\left(\frac{R_\odot}{r}\right)^2 f_\infty(E)\beta(E)c , \tag{2.4}$$

where the differential density of cosmic ray protons is $f(E) = dn/dE$, βc is the velocity, and the subscript N indicates that this is the naive value for a freely propagating flux absorbed on the surface of a sphere of radius $R_\odot$. In a crude attempt to account for modulation by the solar wind we take $f_\infty(E) = f_\oplus(E)$, the observed flux at $r_\oplus$. We use $f_\oplus(E)$ as determined by Webber & Potgieter (1989).

The naive absorption rate is then

$$\Gamma_N = \pi R_\odot^2 f_\oplus \beta c . \tag{2.5}$$

With Γ_N as a guide, we turn to the more complete model of solar absorption. This involves calculating a suppression factor, C_D, for propagation through the IMF and corona, calculating the probability that a cosmic ray incident on the photosphere is absorbed, A, and putting these ideas together to get the full absorption rate, Γ.

2.2.1. *Propagation in the IMF*

Our approach is to model propagation through the IMF as a diffusion problem (Palmer 1982). We concentrate on spatial diffusion and ignore diffusion in the energy of the cosmic rays which may be safely neglected at energies above 1 GeV. We account for energy losses by cosmic rays entering the solar cavity by normalizing the Galactic flux to that observed at Earth.

The motion of charged particles is intimately tied to their interactions with the magnetic fields of the IMF. The magnetic field given in equation (2.2) is nearly radial inside Earth's orbit, so we take the diffusion problem to be spherically symmetric. The spherical diffusion equation is

$$\dot{f} - D'f' - D\left(f'' + \frac{2f'}{r}\right) = \epsilon , \tag{2.6}$$

where ϵ is a possible source term and D is the diffusion "constant." Except near or inside the photosphere there is no absorption or production of cosmic rays, so we have set $\epsilon = 0$ and account for absorption by adjusting the inner boundary condition when solving the diffusion equation.

For a time-independent solution, equation (2.6) simplifies to

$$f'' + f'\left(\frac{2}{r} + \frac{D'}{D}\right) = 0 . \tag{2.7}$$

The inward flux is given by

$$j = -Df' , \tag{2.8}$$

which may be used in equation (2.3) to solve for Γ.

For the diffusion "constant" we consider the form,

$$D(E, r) = D_{\oplus 1}(r/r_\oplus)^\alpha (E/1\ \mathrm{GeV})^\beta . \tag{2.9}$$

In equation (2.9) D is normalized to $D_{\oplus 1}$, its value at $E = 1$ GeV and $r = r_\oplus$. Possible radial and energy dependence of D is parameterized by the exponents α and β. Dimensionally, $D \sim vr$; we express D in units where $c = 1$ and r is in AU.

The parameters $D_{\oplus 1}$, α, β are not well known. Palmer (1982) has reviewed the situation. For $E \lesssim 1$ GeV, $D_\oplus \simeq 0.03\ v/c$ AU with a suggestion for $D_\oplus$ to increase with energy above 1 GeV. Different theoretical considerations suggest $0.5 < \beta < 2$. We will use $D_{\oplus 1} = 0.03$, and concentrate on the choice $\beta = 1$. The problem with this is that for $E \gtrsim 30$ GeV, $D_\oplus > 1$. But D is of order the mean free path to scattering off the IMF, and it does not make sense to apply diffusion in a situation where the mean free path is greater than the size of the system. We therefore require

$$D(E, r) < r/8 \tag{2.10}$$

as a constraint on equation (2.9). The linear relationship to r is necessary to maintain causality as either the inner or outer boundary is moved. The choice of 1/8 as a proportionality constant is motivated by solving the diffusion equation (see below) and requiring that the absorbed flux is no greater than in the naive model.

The radial behavior of D is not well known, either. If D were related simply to the magnetic field strength, then equation (2.2) would suggest $\alpha = 2$. This is probably not a correct picture, as diffusion involves fluctuations in the IMF rather than static configurations. Palmer's review cites three experimental determinations of α in the radial range 1 AU $< r <$ 5 AU. These suggest $\alpha_\parallel = 0.9, 1.4, 1.8$, where $\alpha_\parallel$ is the power law for diffusion along the magnetic field lines. Since these values were derived for much lower energy particles than interest us, they are suspect as a guide. The constraint $D < r/8$ suggests $\alpha \geq 1$. We will concentrate on the relatively conservative choice $\alpha = 2$. It is heartening that no consideration yields a large exponent since larger values of α decrease the inward flux.

To solve the diffusion equation we need two boundary conditions on either the density of cosmic rays or its gradient. For one boundary condition we set $f_\oplus$ equal to its observed value. One might worry that when considering cosmic rays very near the Sun there might be a change in the spectrum of the cosmic-ray flux due to solar wind effects. However, in the force field approximation (Gleeson & Axford 1968; Fisk, Forman, & Axford 1973; Perko 1987), modulation by the solar wind does not significantly alter the spectrum once cosmic rays have penetrated as far as Earth, and in any event we are mostly interested in high enough energy primaries that modulation is not a serious problem.

As stated earlier, we continue the diffusion model down to the bottom of the corona where we impose an absorbtive/reflective boundary condition. First, consider the simplest possibility, that this boundary is fully absorbing. This yields an overestimate of absorption, as most cosmic rays entering the photosphere will be magnetically mirrored before being absorbed. The boundary condition for full absorption is $f_\odot = 0$.

We solve equation (2.7) by setting $y = f'$, integrating to get y, and integrating again to get f. The general solution can be

written as

$$yDr^2 = \text{constant} \tag{2.11a}$$

$$f = f_\odot + y_\odot D_\odot R_\odot^2 I(R_\odot, r)\,, \tag{2.11b}$$

where

$$I(R_\odot, r) = \int_{R_\odot}^{r} \frac{1}{D(r')r'^2}\, dr'\,. \tag{2.12}$$

Note that equation (2.11a) is also required by the conservation of flux. With the boundary conditions $f_\odot = 0$ and $f(r_\oplus) = f_\oplus$, we get the solution

$$y_\odot = \frac{f_\oplus}{D_\odot R_\odot^2 I(R_\odot, r_\oplus)}\,. \tag{2.13}$$

Using equations (2.3) and (2.8) we find the absorbed flux for a fully absorbing boundary

$$\Gamma_A^0 = \frac{4\pi f_\oplus}{I(R_\odot, r_\oplus)}\,. \tag{2.14}$$

We define the diffusion correction as

$$C_D \equiv \frac{\Gamma_A^0}{\Gamma_N} = \frac{4}{R_\odot^2 I(R_\odot, r_\oplus)\beta c}\,. \tag{2.15}$$

Given our constraint on D in equation (2.10) we consider three energy regimes. Define r_0 as the radius where $D(E, r_0) = r_0/8$, and further, define $E_\oplus$ by $r_0 = r_\oplus$ and $E_\odot$ by $r_0 = R_\odot$. The correction for IMF diffusion is then

$$C_D = \begin{cases} \dfrac{4}{\beta c}(1+\alpha)\dfrac{D_\oplus}{r_\oplus}\left(\dfrac{R_\odot}{r_\oplus}\right)^{\alpha-1}\left[1-\left(\dfrac{R_\odot}{r_\oplus}\right)^{1+\alpha}\right]^{-1} & E < E_\oplus \\ \left(\dfrac{4}{\beta c}\right)(1+\alpha)\left(\dfrac{D_\oplus}{r_\oplus}\right)\left(\dfrac{R_\odot}{r_\oplus}\right)^{\alpha-1} & \\ \times\left\{1-\left(\dfrac{R_\odot}{r_0}\right)^{1+\alpha}+\left(\dfrac{1+\alpha}{2}\right)\left(\dfrac{R_\odot}{r_0}\right)^{1+\alpha}\left[1-\left(\dfrac{r_0}{r_\oplus}\right)^2\right]\right\}^{-1} & \\ & E_\oplus < E < E_\odot \\ 1/(\beta c) & E > E_\odot \end{cases} \tag{2.16}$$

2.2.2. *Absorption and Reflection at the Photosphere*

Our model for the absorption coefficient, A, draws a distinction between low- and high-energy primaries. Particles with low rigidity spiral in along field lines until they are mirrored at some depth which depends upon the initial pitch angle of the cosmic ray entering the flux tube. High-energy particles, on the other hand, will not be confined to field lines and may land anywhere on the surface. For simplicity we have made the distinction a sharp one and define a threshold energy E_T, although, in a more realistic model we would expect the average behavior for $E_p \sim E_T$ to interpolate between that for low- and high-energy primaries.

We estimate E_T for protons by comparing their gyroradius to other length scales. For relativistic protons in a uniform field the gyroradius is

$$r_p \simeq 3 \times 10^6 E/B \text{ cm}\,, \tag{2.17}$$

where E is in GeV, and B is the magnetic field in gauss. Setting $r_p = R_\odot$ and $B = 1$ G suggests $E_T \lesssim 2 \times 10^4$ GeV. This would be the energy required so that we could ignore the large-scale bipolar field of the Sun. For our problem, however, we are more interested in the field structure of the canopy, that is, where the flux tubes broaden out and merge. Canopy fields are of order 10 G with horizontal coherence of order 10^8 cm, which suggests $E_T \gtrsim 300$ GeV. We take an intermediate value, $E_T \equiv 3 \times 10^3$ GeV. It is quite possible that particles with E between 300 GeV and 3 TeV diffuse through most of the corona, but penetrate the last part freely, thus avoiding the flux tubes at the surface.

Once a particle finds itself trapped inside a flux tube, it remains trapped until it is mirrored and escapes out the top. Suppose that upon entering the flux tube the gyroradius is less than the diameter of the tube, $r_p < d$. Then, as the tube narrows the total flux, $\Phi \sim Bd^2$, remains constant, which implies $r_p \sim 1/B \sim d^2$. As d decreases, r_p decreases even faster—once trapped, always trapped. This argument supports the use of canopy fields as the criteria for determining E_T. It also justifies treating the magnetic flux linked within a charged particle's gyroradius as an adiabatic invariant, and we use this in calculating the absorption coefficient A, for $E_p < E_T$. For $E_p > E_T$ we simply set $A = 1$.

The geometry of the flux tube (see Fig. 2) is determined assuming that the magnetic field strength within a flux tube is in pressure equilibrium with the ambient gas, and that the gas pressure scale height is the same both inside and outside the flux tube. In the chromosphere we take the temperature to be constant, so $P_{\text{gas}} \sim \rho \sim \exp(-z/h)$ (see eq. [2.1]). Below the photosphere we take the pressure from Baker & Temesvary (1966). This determines the magnetic field strength as a function of height. We take the field strength within a flux tube to be 1500 G at the photosphere and 6.5 G at the top of the tube, corresponding to a canopy height of 1250 km for a scale height of 115 km. These values are consistent with a picture (Spruit 1981) where flux tubes are located at the corners of convective cells, the canopy occurs at a height where the tubes have flared to the point where they overlap, and neighboring flux tubes are almost always of the same sign.

Now, suppose a cosmic ray enters a flux tube at its top with a pitch angle, θ_0, and that the magnetic field strength at the top of the tube is B_0. Using the adiabatic invariance, the pitch angle at depth is $\cos\theta = \sqrt{1 - B/B_c}$, where the critical field is defined by $B_c = B_0/\sin^2\theta_0$. Since $B^2 \sim P$, a cosmic ray injected into a flux tube will be mirrored at a pressure of

$$P_m = P_0/\sin^4\theta_0\,, \tag{2.18}$$

where P_0 is the pressure at the top of the flux tube.

To calculate the absorption coefficient for protons we average over an isotropic flux at the top of a flux tube. For each incident angle, we calculate a trajectory into the flux tube and out. The column density of matter experienced along the path is calculated as $x = \int [n(z)/\cos\theta]dz$. The absorption probability for a given incident angle is then $A(\theta_0) = 1 - \exp(-x\sigma_{pp})$, where $\sigma_{pp} \simeq 33$ mbarn is the inelastic proton-proton cross section. The full absorption coefficient is given by averaging over angles $A = 2\int A(\theta_0)\sin\theta_0\cos\theta_0\, d\theta_0$. For the nominal flux tube parameters given above, we find $A = 5.2 \times 10^{-3}$ for protons and $A = 8.8 \times 10^{-3}$ for ^{4}He nuclei.

In determining A, the path length x is dominated by the integration near the turning point of the orbit. Thus, the uncertainty in the canopy height and shape of the flux tube in the chromosphere does not change the relative probability for absorption at a particular depth, just the overall normalization. Since A measures the size of the loss cone near the vertical, it is easy to rescale A for different flux tube parameters by using equation (2.18) and the relation $B^2 \sim P$:

$$A \sim \sin^2(\theta_0) \sim (P_0/P_m)^{1/2} \sim B_0\,. \tag{2.19}$$

So, for example, if the surface density of flux tubes were increased, the canopy would be lowered, and B_0 would increase, leading to a proportionally greater absorption coefficient.

2.2.3. *The Full Absorption Rate*

In § 2.2.1 we estimated how the IMF affects the rate at which cosmic rays are absorbed by the Sun under the assumption that the photosphere was fully absorbing. In § 2.2.2 we estimated the absorption coefficient of the photosphere and found out that it was small. Here, we put those two ideas together to arrive at a full expression for the absorption rate.

Let the absorption rate for a fully absorbing boundary be Γ_A^0. Then the fraction of that flux that is absorbed is $\Gamma_A^1 = A\Gamma_A^0$, and the fraction that is reflected back into the solar system is $\Gamma_R^1 = (1 - A)\Gamma_A^0$. If the reflected flux escaped freely from the solar system, then the total absorbed flux would be just $\Gamma = \Gamma_A^1$. However, in general only a fraction ϵ of the reflected flux escapes the solar system. The remainder diffuses around in the inner solar system and returns to the inner boundary before it escapes. When this happens there is again a probability A that the flux will be absorbed. This leads to a second contribution to the absorbed flux $\Gamma_A^2 = A(1 - \epsilon)(1 - A)\Gamma_A^0$. The remaining flux is reemitted from the inner boundary and again has a chance to escape. Each time through the cycle the contribution to the total absorbed flux is reduced by $x = (1 - A)(1 - \epsilon)$. The total absorbed flux is then

$$\Gamma = A\Gamma_A^0(1 + x + x^2 + \cdots) = \Gamma_A^0 \frac{A}{A + \epsilon - \epsilon A} . \quad (2.20)$$

Similarly, the total flux that escapes is

$$\Gamma_{\rm esc} = \Gamma_A^0 \frac{\epsilon(1 - A)}{A + \epsilon - \epsilon A} . \quad (2.21)$$

It remains to determine ϵ. We start by assuming that the reflected flux leaves the photosphere isotropically, neglecting that a small fraction of flux has been absorbed from a rather small loss cone near the zenith. In order to have a total outward flux equal to that reflected, Γ_R, we must adjust the cosmic-ray density at the solar surface. The local outward flux is given by

$$2\pi\beta c \int_0^1 \frac{f}{4\pi} \cos\theta d(\cos\theta) = \frac{f\beta c}{4} . \quad (2.22)$$

The total rate at which cosmic rays leave the surface is then $\pi R_\odot^2 f$. Equating this to the reflected flux, the boundary condition at the surface is

$$f_\odot = \frac{\Gamma_R}{\pi R_\odot^2 \beta c} . \quad (2.23)$$

For flux escaping the solar system, the outer boundary condition is $f_\infty = 0$. The flux that escapes (i.e., the *net* flux—not the *total* flux—leaving the surface) is given by

$$\Gamma_{\rm esc} = 4\pi R_\odot^2 D_\odot y_\odot = \frac{4\pi f_\odot}{I(R_\odot, \infty)} = \frac{4\Gamma_R}{R_\odot^2 I(R_\odot, \infty)\beta c} , \quad (2.24)$$

where in the second step we used equation (2.11b). The escape efficiency is then

$$\epsilon \equiv \frac{\Gamma_{\rm esc}}{\Gamma_R} = \frac{4}{R_\odot^2 I(R_\odot, \infty)\beta c} . \quad (2.25)$$

Apart from a small difference between $I(R_\odot, \infty)$ and $I(R_\odot, r_\oplus)$, we find that $\epsilon = C_D$. Using $\epsilon = C_D$, along with the relation $\Gamma_A^0 = C_D\Gamma_N$, in equation (2.20), we get the final expression for the absorbed flux

$$\Gamma = \frac{AC_D\Gamma_N}{A + C_D - AC_D} . \quad (2.26)$$

In Figure 3 we show Γ for protons under various assumptions about particle propagation. The bold curves show the naive absorption rate Γ_N. The solid curve in Figure 3*a* shows Γ for our nominal choice of parameters, $A = 5.2 \times 10^{-3}$ and ($\alpha = 2$, $\beta = 1$, $D_{\oplus 1} = 0.03$). The sharp break at 3×10^3 GeV is due to the discontinuous change in A at $E_p = E_T$. Keeping A fixed and varying the diffusion parameters to a pessimistic ($\alpha = 2.0$, $\beta = 0.5$, $D_{\oplus 1} = 0.01$: *dashed curve*) or an optimistic scenario ($\alpha = 1.5$, $\beta = 2$, $D_{\oplus 1} = 0.1$: *dotted curve*) results in relatively minor changes. If we had used a larger value of A, the effect of varying C_D would be more noticeable since it is the *smaller* of the two quantities that controls Γ. In Figure 3*b* we show the results for our nominal choice of diffusion parameters but allowing the absorption coefficient A to vary.

Note that generally, at $E_p \sim 1$ GeV we find $C_D < A$ and from equation (2.26) C_D controls the absorption rate for these energies. Since our γ-ray and neutron results are sensitive to the magnitude of the low-energy flux, these results depend mostly on the diffusion parameters and not so much on the calculation of the absorption coefficient A. The neutrino yields, on the other hand are more sensitive to the high-energy flux (above 100 GeV) which depends more on our model of absorption, since C_D is nearer unity. Even so, the neutrino results are fairly insensitive to our model for A since a substantial part of the neutrino signal arises from primaries for which $E > E_T$, where we reasonably take $A = 1$.

2.3. *Cosmic-Ray Cascades in the Sun*

In this section we discuss general features of solar cascades, leaving details to discussions of the individual signals. Our attempt to account for magnetic fields in and around the Sun leads us to distinguish between cascades which develop from $E < E_T$ primaries and those with $E > E_T$. As discussed in § 2.2.2 high-energy cosmic rays may land anywhere on the solar surface, whereas for $E < E_T$ the primaries are confined to interact with matter inside the magnetic flux tubes.

By assumption, primaries with $E_i > E_{T_i}$ do not follow the magnetic field lines into the high field flux tubes. For the moment let us treat the intertube regions as if they are field free and estimate how far primaries penetrate into the Sun. The inelastic cross section for cosmic-ray collisions per baryon is $\sigma_{\rm pp} \approx 33$ mbarn. Combining this with the solar atmosphere described in § 2.1 a proton moving vertically downward has an optical depth to absorption of one at a depth where $x \equiv \int^z \rho/m_p dl \approx 1/\sigma_{\rm pp}$. This occurs for z about 500 km below the photosphere. Now, suppose that there was a residual magnetic field of order 1 G in the intertube regions. The gyroradius for an $E_p = E_{T_p}$ proton would be $\sim 10^{10}$ cm, approximately 200 times the interaction depth. We conclude that magnetic fields do not affect the zenith angle distribution of high-energy primaries. Furthermore, they do not affect the geometrically

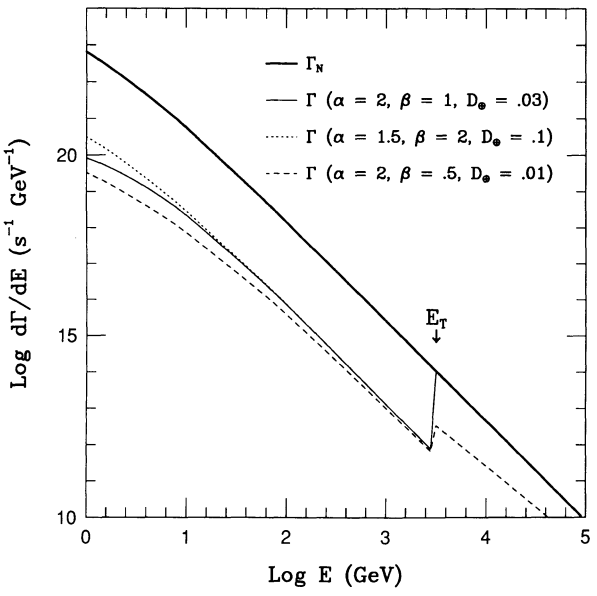

FIG. 3a

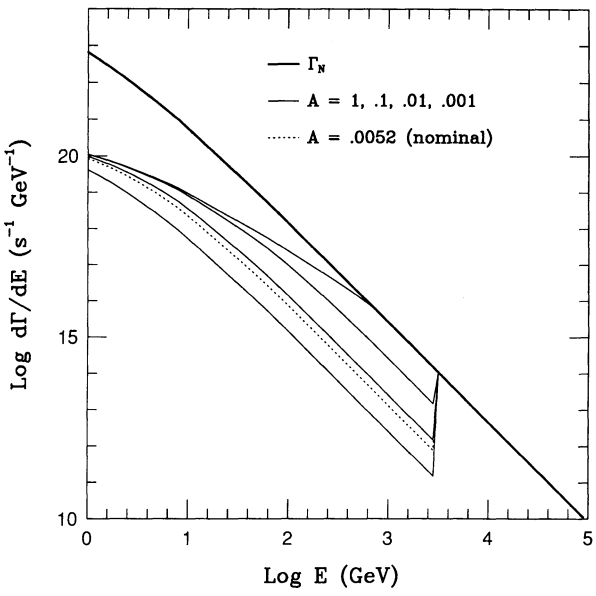

FIG. 3b

FIG. 3.—Absorption rate of cosmic rays by the Sun for different assumptions about cosmic-ray transport. (*a*) Varying assumptions about diffusion in the interplanetary magnetic field. (*b*) Varying the absorption coefficient of the photosphere, *A*. In both, the bold curve shows the naive result (ignoring magnetic fields) which is an absolute upper limit. In (*a*) our nominal case is shown as a solid line, while in (*b*) it is shown as dotted.

linear development of the cascade until particle energies are below $\sim$10 GeV. By this time, most cascades will be deep enough that few low-energy photons or hadrons will escape. Although some may escape for primaries that graze the surface, in general we expect the escape probability for photons and baryons from high-energy cascades to be quite small. Neutrinos, however, may escape from any depth, and so our neutrino yields must include the high-energy cascades.

For the high-energy cascades it is also important that the scale height of the solar atmosphere is 10 times or more that of Earth. Further, there is no surface below the atmosphere to sharply curtail cascade development. Both these effects increase the probability that a meson of given energy will decay (producing neutrinos) before it interacts with the surrounding medium.

In our model, low-energy cascades, $E < E_T$, take place within the magnetic flux tubes. We calculate the initial interaction sites and zenith angles by tracing the paths of the incoming primaries, as outlined in § 2.2.2. Many of the interactions take place after the primary has been mirrored, and these may generate a substantial albedo flux of γ-rays and baryons. Even if the primary interaction takes place on a downward trajectory, the charged particles in the cascade will still be mirrored, and so even these cascades may produce some albedo.

Together, the above remarks lead to a qualitative difference between high- and low-energy cascades. The high-energy primaries initiate thick target cascades, that is, since they travel in straight lines, the cascade would have to pass through the whole Sun for baryons and photons to escape. The only particles to escape from a thick target cascade will be neutrinos. The low-energy primaries, on the other hand, produce cascades where a significant amount of energy is reflected back to the solar surface. The typical low-energy cascade, has less than a few interaction lengths of material to pass through before photons and neutral baryons can escape. Thus, for γ-ray production these cascades act as if they evolve in moderately thin targets.

3. NEUTRINOS

We begin our discussion of possible signals by considering high-energy neutrino production (Gaisser & Stanev 1985). The neutrinos are observed through the production of leptons in charged current events. We are mostly concerned with the production of muon neutrinos. They are easier to detect since muons have small energy losses and long ranges compared to electrons, so a detector of a given size is more sensitive to muon neutrinos than to electron neutrinos.

We treat the Sun as a point source of neutrinos since the solar disk is not resolvable with any operational or planned neutrino telescope. We will also assume that the neutrino flux is isotropic, that is, as emitted by the Sun. The incident flux of Galactic cosmic rays is nearly isotropic (Hillas 1984) and, as discussed in § 2.3, the high-energy cascades develop linearly, so we expect the neutrino yield to be isotropic as well. For lower energy cosmic rays anisotropy could result from a number of mechanisms, but since the neutrino signal would be dominated by higher energy neutrinos, we will postpone a discussion of anisotropy until the section on γ-rays.

With these assumptions the neutrino flux at Earth is simply related to the total neutrino luminosity,

$$\frac{d\phi}{dE_\nu}(E_\nu) = \frac{1}{4\pi r_\oplus^2}\frac{dL_\nu}{dE_\nu}, \tag{3.1}$$

which in turn is determined from the absorbed cosmic-ray flux by

$$\frac{dL_\nu}{dE_\nu}(E_\nu) = 2\int_0^1 \sum_i \int_{E_\nu}^\infty y_\nu(E_\nu, E_i, z)\Gamma(E_i)dE_i\, z\, dz\,. \tag{3.2}$$

In equation (3.2), the sum over i includes both p and ^{4}He primaries, $y_\nu(E_\nu, E_i, z)$ is the differential neutrino yield from a

primary of energy E_i which enters the Sun with zenith angle θ, and $z \equiv \cos(\theta)$. By using equation (3.2) we implicitly assume that all cascades develop linearly. In fact, primaries with energies between E_ν and E_{T_i} produce cascades inside the magnetic flux tubes and do not develop linearly. However, these primaries do not dominate the production of the underground muons by which the neutrinos are detected at Earth, and so we make only a small error. For photons, § 4, we will deal more carefully with $E_i < E_{T_i}$ primaries.

We average over zenith angle to account properly for the hadronic interactions of pions and the electromagnetic stopping of muons. As stated in § 2, the scale height of the solar atmosphere is greater than Earth's and as a result these effects are not as severe as in terrestrial cascades. In Earth's atmosphere a pion will decay before it interacts if $E_\pi \lesssim 200$ GeV, but in the solar atmosphere the equivalent energy is 10–50 times as great, depending upon where the proton is absorbed. For $E_\pi < 10^4$ GeV most charged pions decay and produce a neutrino and a muon, but above that energy only a fraction $\sim 10^4\ \mathrm{GeV}/E_\pi$ decay.

For muons, the primary effect of the medium is electromagnetic stopping, which we approximate by

$$\frac{dE}{dx} = \rho(\epsilon_0 + \epsilon_1 E)\,, \tag{3.3}$$

where $\epsilon_0 \simeq 0.007$ GeV cm^2 g^{-1} and $\epsilon_1 \simeq 1.8 \times 10^{-6}$ cm^2 g^{-1} at $E = 1$ TeV for a gas which is 72% hydrogen and 28% helium by mass (Lohmann, Kopp, & Voss 1983). Muons require an exponentially large energy to penetrate to column depths greater than $\sim 5 \times 10^5$ g cm^{-2}. For vertical muons this corresponds to a depth of 1.3×10^9 cm, or an initial energy of $\sim 2 \times 10^3$ GeV to penetrate this far before decaying. Coincidentally, this is also of order the energy loss from the first term in equation (3.3). In generating neutrino yields from $E_i > E_{T_i}$ primaries we include the effects of muon energy loss.

There are a few other aspects of the high-energy cascades which we mention. Neutrinos (antineutrinos) with $E_\nu \gtrsim 100(150)$ GeV which pass through the core of the Sun may be absorbed. Absorption is not negligible for higher energy neutrinos passing at less than 0.5 $R_\odot$ from the center of the Sun, and it is properly accounted for in this calculation. The absorption reduces the neutrino-induced muon flux by about 15%, the exact factor depending on the threshold energy for detecting the ν-induced muons at Earth. We also note that since the effects of the medium are slightly less severe for pions than muons, most high-energy muon neutrinos come from π-decay, as in terrestrial showers. For electron neutrinos there is also an enhancement over terrestrial cascades; however, as in terrestrial cascades, most ν_e's derive from muons, which have longer lifetimes than pions and are less likely to decay before stopping. Thus the flux of ν_e's is intrinsically less than for ν_μ's.

The calculated neutrino flux is shown in Figure 4. The bold curve uses the naive model for Γ_N described by equation (2.5). This is an absolute upper limit. The light curve shows our nominal result assuming the light solid line in Figure 3*a* for the absorbed flux. Also shown in Figure 4 is the angle-averaged background flux (*dotted*) from neutrinos produced by cosmic rays in Earth's atmosphere (Volkova 1980). The background is shown for an angular disk of 6.8×10^{-5} sr, the size of the Sun, although this should be increased accordingly to account for the angular resolution for a specific experiment. The flux using the naive Γ_N is always brighter than the background, and the

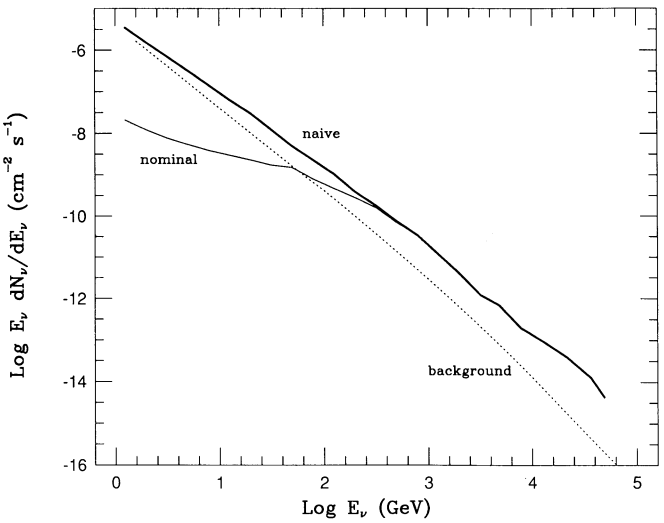

FIG. 4.—Neutrino flux at Earth for different assumptions about cosmic-ray transport. The bold curve shows an upper limit using the naive absorption rate shown as the bold curve in Fig. 3. The solid curve gives our nominal result. The background from terrestrial cosmic-ray cascades is shown for a solid angle equal to the size of the Sun's disk.

ratio increases with energy up to $\sim 10^4$ GeV. This is the effect of the larger scale height of the solar atmosphere. For the more realistic, nominal propagation model the flux is lower than the background for $E_\nu \lesssim 50$ GeV, but rises up to the naive value by $E_\nu \simeq 200$ GeV, which is the typical energy for neutrinos arising from primaries with $E = E_T$; recall that for $E > E_T$ our model assumes $\Gamma = \Gamma_N$.

The most probable means of detecting the neutrino flux would be to look for muons produced in charge current interactions in rock or water. If the muons pass through two or more sensitive planes in an upward direction, then they can be distinguished from "punch through" muons produced in terrestrial air showers, and a direction pointing back to the Sun can be determined. The flux of muons that results from our calculations (Gaisser & Grillo 1987) is shown in Figure 5. The curves are labeled as in Figure 4. We show the integrated flux above a threshold energy since that is most closely related to the experimentally measured quantity. Here the nominal signal is greater than the background even at low energies since much of the signal comes from higher energy neutrinos. There are, however, physical limitations on the angular resolution of muon telescopes. The muon direction differs from the neutrino direction by $\sim 10\sqrt{10\ \mathrm{GeV}/E_\mu}$ degrees, and this will limit resolution if the production vertex is not observed. For low-energy muons, multiple scattering at the end of their path will also limit the resolution. It is conceivable that a very large detector would be capable of cutting on only high-energy, contained events; but generally we expect that the background in Figure 5 should be increased to account for detector resolution. So, for example, a detector with an area times efficiency of 10^8 cm^2 and a threshold of 10 GeV would yield an event rate of $R \simeq 0.15$ yr^{-1}. For example, the proposed GRANDE (Adams et al. 1990) and DUMAND (DUMAND 1988) detectors have effective areas a few times this size and would see less than 1 signal event per year. Given a comparable number of background events within the angular resolution (1°) it would take decades to identify a signal; so for the moment, we conclude that the solar cascade neutrino flux is unobservable.

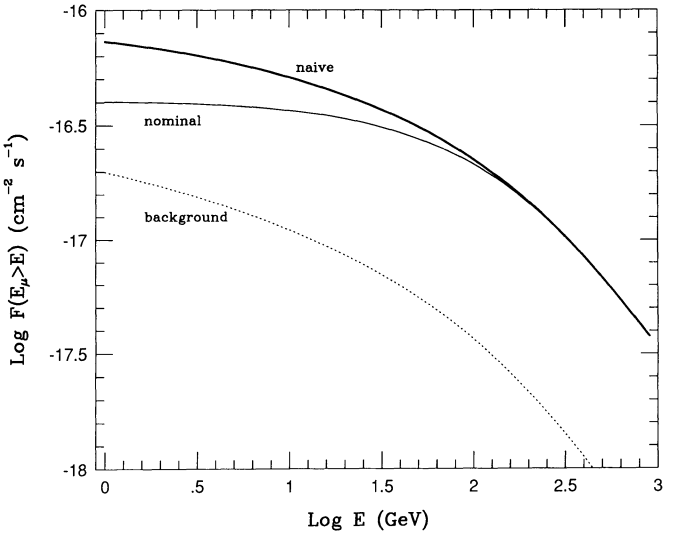

FIG. 5.—Underground muon flux from solar albedo neutrinos, integrated above a threshold energy, E. The curves are for the same models as in Fig. 4.

Finally, a reason for considering the solar cascade neutrino flux was the worry that it might be a bothersome background to searches for neutrinos from dark matter annihilation in the Sun. Current limits (Sato et al. 1990; Losecco et al. 1987; Casper 1990) are on the order of 10^{-14} muons cm^{-2} s^{-1}, more than two orders of magnitude larger than our calculated background. Nonetheless, a truly large neutrino telescope will close that gap. Further, as accelerator experiments continue to push particle dark matter properties, rates as low as 10^{-16}–10^{-17} cm^{-2} s^{-1} are being discussed (Kamionkowski 1990; Seckel 1990), and so, although solar cascade neutrinos are not important yet, they may soon be a limiting factor to this indirect method of searching for dark matter.

4. GAMMA RAYS

The best opportunity for an observable signal comes from photons produced in the solar cascade. These may arise either from two photon decays of π^0's or from the electromagnetic shower in the latter part of the cascade. For the moment we treat the Sun as an isotropic point source.

The γ-ray flux at Earth is given by

$$\frac{d\phi}{dE_\gamma}(E_\gamma) = \frac{1}{4\pi r_\oplus^2}\frac{dL_\gamma}{dE_\gamma}, \tag{4.1}$$

where the γ-ray luminosity of the Sun is given by

$$\frac{dL_\gamma}{dE_\gamma}(E_\gamma) = \sum_i \int_E^{E_{T_i}} Y_i(E_\gamma, E_i)\Gamma_i(E_i)dE_i\,. \tag{4.2}$$

The sum over i includes both p and ^{4}He primaries, and Γ_i is given by equation (2.26). The γ-ray yield per absorbed primary of energy E depends upon the path length x, the amount of matter between the interaction site and empty space. We therefore average over the path length distribution

$$Y_i(E_\gamma, E_i) = \int y_{\gamma i}(E_\gamma, E_i, x)\frac{dP_i}{dx}\,dx\,, \tag{4.3}$$

where $y_{\gamma i}$ is the yield of photons of energy E_γ that result from cascades with path length x initiated by primaries of energy E_i, and dP_i/dx is the probability that a primary of species i produces a cascade with path length x. In separating $P_i(x)$ and $\Gamma_i(E)$ we have ignored the slow energy dependence of the hadronic cross section in determining the initial interaction site. We do, however, include this energy dependence in the Monte Carlo calculation of the yields, $y_{\gamma i}$.

Unlike the case for neutrinos, we do not include $E_i > E_{T_i}$ since most of these cascades develop along straight lines and, although a few primaries just grazing the Sun will have small x, most will have large x, that is, they develop in a "thick" target and will produce very few albedo photons. For $E_i < E_{T_i}$ magnetic mirroring leads to a high probability for $x \lesssim 100$ g cm^{-2}, and these "thin" target cascades produce a substantial albedo. In the intermediate region there is presumably some energy-dependent loss of albedo due to cosmic rays that miss the flux tubes and do not mirror.

It remains to calculate the path length distribution dP_i/dx. If we neglected the charged nature of cascades, we would calculate x by multiplying the vertical column density $x_{\rm vert}$, by $1/|\cos(\theta)|$, where θ is the zenith angle of the primary trajectory at the interaction site. In this limit, only primaries that interact *after* they are mirrored contribute to the albedo. However, as pointed out in § 2, a good fraction of the energy in the cascade consists of charged particles, and since the evolution of the pitch angle with depth does not depend on a particle's energy, the cascade tends to follow the same path the primary would have followed had it not interacted. The cascade will not follow the primary path exactly since some of the energy is neutral and not reflected by the convergent field, but there is still a substantial contribution to the photon albedo from primaries that interact *before* they are mirrored.

To explore this issue in the extreme, we use two models for x. The first calculates x assuming the cascade is neutral and uses $x = x_{\rm vert}/|\cos(\theta)|$. The second uses a column depth given by integrating along the primary particle trajectory as if all cascade particles were charged. Note that this is always of order the interaction column depth of the primaries, even for cosmic rays with $\cos\theta > 0$ at the interaction site. In principle, we could have written a new Monte Carlo to perform a more careful treatment of cascade development in the magnetic environment, but by considering two extreme cases we bound the errors, and given the other uncertainties this seemed acceptable. In Figure 6 we show dP/dx and $I(x) = \int_0^x (dP/dx')dx'$ [normalized to $I(\infty) = 1$] for protons, for the two models. The solid curves illustrate the first case, and the dashed ones the second. Note that most of the cascades are produced with $\cos\theta > 0$ (i.e., downward) and these are not included for the first case.

As regards the sensitivity of dP/dx to the model of the flux tubes, most absorption occurs near or below the photosphere, so there is little sensitivity to details of how the flux tubes flare out and merge at the canopy—apart from an overall normalization which may be accounted for in the absorption coefficient, A. On the other hand, we have assumed that flux tubes maintain their simple vertical geometry below the photosphere. Since this assumption may be questioned in the turbulent environment of the upper convective zone, we acknowledge some uncertainty in dP/dx. However, it seems likely that cool gas descends from the corners of convective cells in strong downdrafts (Spruit 1981; Nordlund & Stein 1990), and we expect that this will tend to make the flux tubes vertical.

The actual yields are calculated by propagating one-dimensional cascades through a slab of column depth x. We

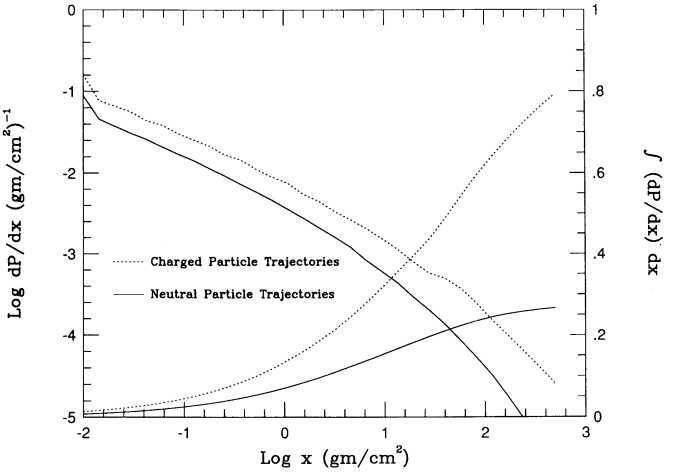

FIG. 6.—Path length distribution for cascades initiated by low-energy (1 GeV < E < 3 TeV) cosmic-ray protons in photospheric flux tubes. Path length, x, is the column depth experienced by cascade products which escape the Sun from the primary interaction site.

include all relevant baryonic interactions and electromagnetic processes for γ-rays, e^+'s, and e's. Our cascade program includes meson interactions and electromagnetic stopping even though the rates for these processes are much slower than the decay rates at the relevant energies and densities, and consequently almost all mesons decay in flight.

The photon yield includes only the photons that make it through the slab. Secondary electrons, positrons, and baryons exiting the slab are thrown away even though it is likely that they will reenter the Sun to be absorbed rather than diffusing off to infinity. Thus, our results may underestimate the actual γ-ray flux by a substantial factor (perhaps 3 or 4). Note, however, that primaries which escape without interacting are implicitly accounted for by our treatment of the full absorption rate. Also, because of the one-dimensional nature of our cascade we do not properly account for γ-rays emitted backward from relatively slow π^0's. The maximum overestimate is a factor of 2 at photon energy $E_\gamma = m_\pi/2$ and becomes negligible for $E_\gamma > 200$ MeV. In addition we do not account for the energy-dependent loss of albedo near E_{T_i}. We do not consider this a serious problem since the major contribution to the γ-ray flux above 100 MeV comes from primaries below 100 GeV.

The calculated differential and integrated photon flux is given in Figures 7 and 8, respectively. In each figure, the two sets of curves correspond to naive (*bold*) absorption by the Sun and absorption assuming our nominal (*light*) assumptions about diffusion in the IMF and corona. In each set the lower curve is the albedo for (1) the slant depth model, and the upper curve is the albedo assuming (2) showers are mirrored as charged particles would be. The dotted curve in Figure 7 shows the expected background of γ-rays from the Galaxy. Above 100 MeV the background is mostly due to cosmic-ray collisions with intergalactic gas, which we estimate by using the spectral shape of Dermer (1986) normalized to the *SAS* 2 data (Fichtel et al. 1977). For lower energies we use a fit to the *SAS* 2 data which includes both a disk and a halo component. The background is shown for Galactic latitude, $b = 30°$. The Sun has $b > 30°$ approximately 61% of the time. Both signal and background are given for a disk the size of the Sun and so, to compare signal to noise one must increase the background to account for angular resolution of the detector.

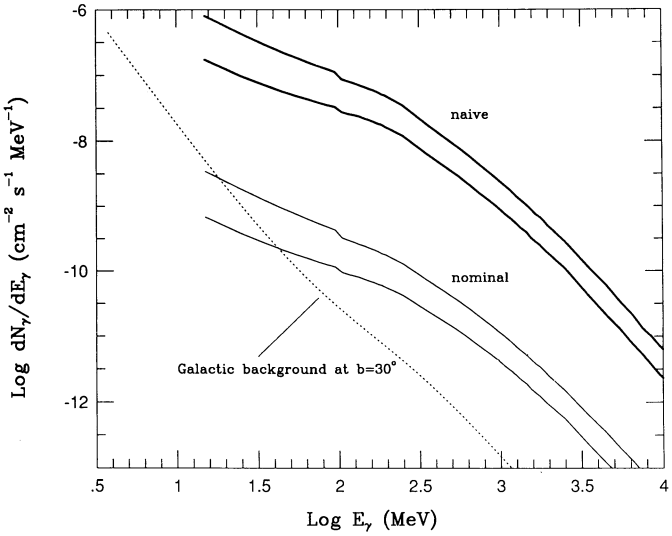

FIG. 7.—Differential photon flux at Earth for different assumptions about cosmic-ray propagation. Weighting of the curves is the same as in Fig. 4: bold for naive, light for nominal. In each pair of curves the upper curve shows the γ-ray albedo assuming charged particle trajectories for the cascade development, and the lower curve shows the result for neutral particle trajectories. The dotted curve shows the Galactic background for a disk the size of the Sun.

The signal is larger than the Galactic background for reasonable assumptions about cosmic-ray absorption. The counting rate for a 1000 cm^2 detector would be $\sim$2–8 counts per day for photons with $E_\gamma > 100$ MeV. The EGRET instrument of the Gamma Ray Observatory has area times efficiency of order 1000 cm^2 and should be able to detect this signal.

The results in Figures 7 and 8 assumed the Sun to be an isotropic, point-like source. For neutrinos this assumption is fairly benign, but it may not be valid for γ-rays. Anisotropy in the photon flux could result if the absorption rate of cosmic rays by the Sun varies with latitude or, for short time scales, with longitude. Considering the complex connection between surface fields and the interplanetary fields it is easy to imagine that the absorption rate is not constant. Anisotropy could also

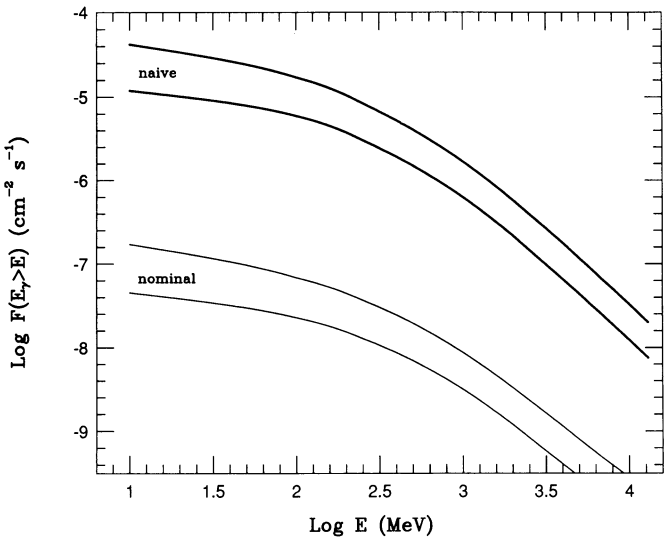

FIG. 8.—Same as Fig. 7, except the integral photon flux is shown

arise if the details of our flux tube model were assumed to be different in, for example, the polar and equatorial regions.

The effects of differential absorption could be modified by the details of producing the photon albedo. For example, many of the observable photons come from cascades that have developed through a few radiation lengths and have been mirrored out of the flux tubes. Such cascades tend to produce beams of photons that are columnated along the flux-tube axis, which is presumably near local vertical. If cosmic rays were absorbed chiefly in the solar polar regions, a beaming effect would lead to a dearth of γ-rays observable from the ecliptic.

A different perspective on the source of photons suggests exactly the opposite effect. For a given incident angle, cosmic rays are mostly absorbed at their deepest penetration. Not coincidentally, this is just where they are mirrored, and thus the local velocity is horizontal. If photons can escape from the interaction site without further interactions, then this process would result in a fan of photons instead of a beam. If cosmic rays are absorbed mostly at the poles, then a fan effect would enhance the signal for ecliptic observers. From Figure 6 we see that about one-half of all interactions take place with path lengths of less than 10 g cm^{-2}. Since this is significantly less than a radiation length, this suggests that the fanning effect may be dominant; however, we feel a full simulation is necessary to answer this question, and this goes beyond the scope of the present paper. The same issue crops up in discussions of γ-ray production in solar flares (Chupp 1987). It is observed that flares occurring on the limb of the Sun are brighter in γ-rays above 10 MeV than those of comparable strength occurring in the center of the solar disk. This also suggests that the fanning effect is more important, but the comparison may be misleading since the source of the >10 MeV flare γ-rays is presumably electrons accelerated in the corona which penetrate down to the photosphere, whereas most of our γ-rays have a source below the photosphere.

5. BARYONS

The third possible signature of cosmic-ray interactions with the Sun would be baryon production. The conversion of high-energy protons and helium nuclei into lower energy protons is distinctly uninteresting, but the production of antiprotons, neutrons, or antineutrons is worth discussing.

5.1. *Antiprotons*

As mentioned in the introduction, the observed flux of cosmic-ray antiprotons remains a tantalizing problem for cosmic-ray theorists. The simplest models hypothesize $\bar{p}$ production via collisions between high-energy cosmic-ray hadrons and interstellar gas. These models predict a flux of $\bar{p}$'s which is roughly a factor of 4 less than that observed around an energy of 10 GeV (Stephens & Golden 1987; Gaisser & Schaefer 1991). Many explanations for this discrepancy have been forthcoming, but none are compelling. Here, we show that antiprotons produced at the Sun cannot explain the discrepancy.

At first, this may seem rather obvious. Of order 5% of cosmic-ray protons interact on Galactic gas before escaping the Galaxy. If a beam of cosmic rays were fully absorbed, it would locally produce a much higher flux of $\bar{p}$'s than predicted in the simple models. However, a beam absorbed on the Sun would result in a flux at Earth diminished by $\sim(R_\odot/1\ \mathrm{AU})^2$, which more than compensates for the enhanced absorption. The caveat is that the influence of magnetic fields might somehow enhance the $\bar{p}$-flux.

The escaping antiprotons can be treated in the same way as the escaping protons were in § 2.2.3. We rewrite equation (2.11b) as

$$\bar{f}_\oplus = f_\infty + y_\odot D_\odot R_\odot^2 I(r_\oplus, \infty) = \frac{\Gamma_{\rm esc}}{4\pi} I(r_\oplus, \infty)\,, \quad (5.1)$$

where the outer boundary condition is $f_\infty = 0$ and we use $yDr^2 = \Gamma_{\rm esc}/4\pi$. Equation (2.24) gives $\Gamma_{\rm esc}$ except that the injected upward flux is not given by $\Gamma_R = (1 - A)\Gamma_A^0$, but by $\Gamma_{\rm inj} = y_{\bar{p}}(\bar{E}, E)\Gamma_A$, where $y_{\bar{p}}$ is the antiproton yield and $\Gamma_A(E)$ is the absorbed proton flux given by equation (2.26). Finally, to simplify our discussion we use yields averaged over the absorbed spectrum, and pretend that protons with energy E give rise to antiprotons with average energy $\bar{E} = zE$. As an estimate, $\bar{E} = 10$ GeV, $z = 0.1$, and $E = 100$ GeV, but this choice does not affect our argument. The antiproton spectrum is then

$$\bar{f}_\oplus(\bar{E}) = y_{\bar{p}}(\bar{E}, E)\,\frac{A\epsilon}{(\bar{A} + \bar{\epsilon} - \bar{A}\bar{\epsilon})(A + \epsilon - A\epsilon)}\,\frac{\bar{I}(r_\oplus, \infty)}{\bar{I}(r_\odot, \infty)}\,f_\oplus(E)\,, \quad (5.2)$$

where barred quantities refer to antiprotons and unbarred quantities refer to their proton cosmic-ray progenitors. The quantities A, ϵ, and I have the same meanings as in § 2.2.3. For our model of absorption in the photosphere, $\bar{A} \simeq A = 0.005$, and the second factor in equation (5.2) is always less than 1. The next factor is limited to $\bar{I}(r_\oplus, \infty)/\bar{I}(r_\odot, \infty) \le (R_\odot/r_\oplus)^2$, where the equality obtains when the radial dependence of the diffusion constant is $\alpha = 1$, but the ratio is smaller when $\alpha > 1$.

In a similar way, the flux of $\bar{p}$'s at Earth produced in collisions between cosmic rays and interstellar gas is

$$[\bar{f}_\oplus(\bar{E})]_{\rm gal} = y_{\bar{p}}(\bar{E}, E) P_{\rm int} f_\oplus(E)\,, \quad (5.3)$$

where the probability for a proton to interact before escaping the Galaxy is $P_{\rm int} \sim 0.05$. Comparing the Galactic and solar antiproton fluxes we see that the effects of the IMF can only reduce the naive estimate. In fact the argument is even stronger since we have neglected the absorption of antiprotons in the Sun, which will reduce $y_{\bar{p}}$ relative to that for hadronic collisions in the Galaxy.

The Sun is not an efficient source of antiprotons and will not contribute significantly to any excess over expectations.

5.2. *Neutrons*

The second baryonic possibility is neutrons. Neutrons are notorious for their instability: there is no Galactic background to speak of. Since the distance to the Sun, 1 AU = 500 light-seconds, is comparable to the neutron lifetime, $\tau_n = 888.6 \pm 3.5$ s (Aguilar-Benitez et al. 1990), neutrons or antineutrons (see below) produced on the Sun have a good chance of reaching Earth before they decay. The fact that neutrons are not confined by magnetic fields has two implications for us. First, their flux at Earth is given by their yield and simple geometric considerations. Second, a neutron produced on an upward trajectory is not likely to be confined and absorbed in the solar atmosphere.

The calculation of the neutron flux at Earth then follows the same general lines as for photons and neutrinos. The major difference is that most of the neutron yield does not come from the production of secondaries in the collision. Rather, it arises directly from the baryonic material in the incident beam—neutrons bound in ^{4}He may be liberated in spallation reac-

tions. In addition, incident protons (bound or unbound) with $E \gtrsim 300$ MeV may convert to neutrons in charge exchange interactions involving pion production. In fact, below a few GeV pion production is dominated by Δ resonance production which peaks at incident energy of order 600 MeV. Combining the rapid decrease of primary flux with energy and the threshold for pion production one expects that neutron production is dominated by spallation of incident ^{4}He. There is a third source of neutrons, those locked up in target ^{4}He. These may be released with relatively high energy if a struck nucleon emerges at high energy as a neutron; however, soft spallation neutrons from target ^{4}He nuclei are generally too low in energy to survive neutron decay until they reach Earth.

Due to the importance of ^{4}He spallation as a neutron source, we have constructed a separate Monte Carlo to model neutron production. This Monte Carlo is described in detail in the Appendix—here it suffices to note that it includes spallation of target ^{4}He, incident ^{4}He, and possible compound fragmentation products. The Monte Carlo program also explicitly includes charge separation in the development of the cascades. We used the new program with the incident flux of protons and ^{4}He taken from our nominal propagation model. The flux of neutrons at Earth, accounting for neutron decays in 1 AU, is shown in Figure 9. The contributions from incident ^{4}He and protons are shown separately, and the helium contribution may be seen to be the most important.

We calculate an integrated flux above 100 MeV of I_n(100 MeV) $\sim 2.3 \times 10^{-8}$ cm^{-2} s^{-1}. Whether or not this flux could be detected, we do not know. Upper limits to the quiet time flux are (Lockwood 1973) I_n(100 MeV) $\lesssim 10^{-3}$ cm^{-2} s^{-1}, but these limits are some twenty years old. Although these limits may have been improved upon incidentally by instruments such as the Gamma-Ray Spectrometer (GRS) on the *Solar Maximum Mission* (*SMM*) satellite, we know of no definitive analysis. By way of comparison, neutrons produced during large solar flares have been detected by the GRS (Chupp et al. 1987). The integrated flux associated with the flare of 1982 June 3 was $>10^{30}$ neutrons with $E > 100$ MeV, which corresponds to ~ 200 yr of our predicted quiet time flux.

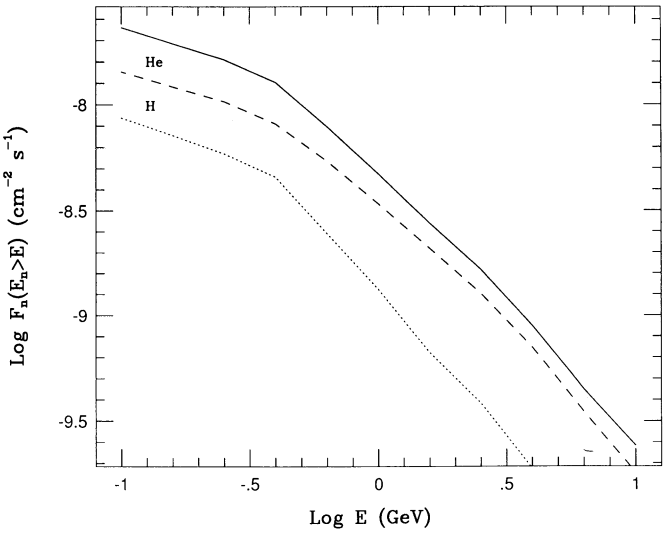

FIG. 9.—Neutron flux at Earth due to cosmic-ray interactions in the Sun. The dotted (*dashed*) curve shows the production due to incident protons (^{4}He). The contribution from ^{4}He is due mostly to spallation of incident nuclei, whereas incident protons contribute through inelastic process at higher energies and target spallation at lower energies.

As the previous paragraph suggests, it would be extremely difficult to detect the neutron flux we propose. The chief problem would be separating out the backgrounds due to terrestrial cosmic-ray albedo neutrons (tCRAN), Galactic γ-rays, and charged particles that enter the detector. In near-Earth orbit the tCRAN flux produced by protons just grazing the atmosphere is about 10 times the quite time solar flux limits (Lockwood 1973) for $E \sim 100$ MeV. Thus, one would have to separate out the solar cosmic-ray albedo neutrons (sCRANs) from the tCRANs at the level of 1 part in 10^5. Galactic γ-rays would also be a problem unless the detector had either good angular resolution or good event identification. For example, a cone of 5° radius would contain an estimated flux of γ-rays above 100 MeV $\sim 10^{-6}$ cm^{-2} s^{-1}; about 40 times our predicted neutron flux. Perhaps most difficult would be understanding the background from cosmic-ray protons. Even with a good veto for charged particles there would probably be events that mimicked solar neutrons. These would have to be discriminated against at the level of $\sim 10^{-7}$, assuming the primary flux $f_\oplus$ in § 2.

Even if other particle backgrounds can be eliminated, one might have to deal with other sources of solar neutrons, such as those produced in flares. In fact, in anticipation of such sources, detectors with several hundred cm^2 of sensitive area have been proposed (Frye et al. 1988). Such a detector would generate an event per day from our proposed quiet time flux, and so, despite the background problems, it is not completely obvious that a quiet time flux could not be observed.

5.3. *Antineutrons*

The third baryonic signature that we contemplate is antineutrons. We do not know of any relevant experiments. Antineutrons, like antiprotons, can only be produced in the fragmentation of the hadronic jets. Like neutrons, once outside the photosphere they should easily escape to Earth orbit. The antineutron yield per collision may be approximated by taking the antiproton yield in hadronic collisions above 10 GeV. This is of order 0.1 per collision, whereas the neutron yield is ~ 1 per event. We therefore expect a $\bar{n}$ yield of order 10% the n yield for $E_{\bar{n}} \gtrsim 5$ GeV which gives an integrated flux of about 6×10^{-10} cm^{-2} s^{-1}. If there is difficulty separating n's and $\bar{n}$'s, then the solar production of neutrons would be an inpenetrable background. Although nonrelativistic $\bar{n}$'s could be distinguished by the annihilation signal, the kinematics of the production event suppresses low-energy antineutrons. For high-energy $\bar{n}$'s, annihilation would not provide a useful signal. If antineutron events could be identified, then the only obvious background would be terrestrial albedo antineutrons (CRA$\bar{N}$), but we do not wish to get bogged down in this discussion.

6. SUMMARY AND DISCUSSION

We have estimated the flux of neutrinos, photons, and neutrons at Earth due to particle cascades initiated in the solar atmosphere by Galactic cosmic rays. In order to achieve this we (1) constructed a model of cosmic-ray transport in the inner solar system, and (2) performed Monte Carlo calculations to model the cascade development in the solar environment.

Our results give a flux of γ-rays which should, for our nominal assumptions, be detectable using the EGRET instrument of the Gamma Ray Observatory (Kanbach et al. 1989). Previous estimates of the solar γ-ray albedo have been made in

analogy to the terrestrial cosmic-ray albedo (Hudson 1989). Our nominal flux is slightly larger than those estimates, but the similarity must be considered coincidental since there are two large differences between the calculations. First, we have included the effects of the interplanetary magnetic field in propagating the primary flux of cosmic rays to the Sun, using a diffusion approach to the problem. This decreases considerably the primary flux for energies $\sim$GeV. Second, we argue that the strong magnetic fields near the solar surface result in a substantial albedo for those cosmic rays which interact with the solar atmosphere. By comparison, the terrestrial albedo is quite small—for the high energies considered in this paper it is constrained by geometry to those cosmic rays which graze Earth's atmosphere. At lower energies backscattering in the upper atmosphere also contributes.

Our predicted neutrino flux would yield a muon flux deep underground (or water) of $\sim 4 \times 10^{-17}$ cm^{-2} s^{-1}. This muon flux is probably undetectable in the next generation of neutrino telescopes, for example, GRANDE (Adams et al. 1990) or DUMAND (DUMAND 1988). Both these detectors have areas of a few times 10^8 cm^2, and so would generate only a fraction of an event per year. Further, although the source is brighter (per solid angle) than the background from terrestrial air showers, the angular resolution of both detectors is several times larger than the disk of the Sun. One can hardly consider the neutrino flux to be "detectable" unless experimental angular resolutions improve and a *very* large detector is built.

We have also considered baryonic fluxes, specifically neutrons and antimatter. The neutron flux is detectable in principle, if one considers just raw flux and plausible detector sizes. The problem comes in discriminating against background due to terrestrial albedo neutrons and Galactic γ-rays. The antiproton flux is expected to be less than that from the Galaxy. The antineutron flux is a fairly unique signature of the process we consider, but we do not see how to differentiate between 5–10 GeV antineutrons and other neutral particle fluxes.

Most of our results are sensitive to the assumptions we made concerning cosmic-ray transport in the inner solar system. We broke the problem into two zones—the corona and IMF, and the region near the photosphere. We treated propagation in the outer region as a diffusion problem, with parameters chosen with an eye toward theory and scanty data collected at or outside of 1 AU. The effects of diffusion are summarized in the quantity C_D. For the inner region, we used a flux-tube model of the magnetic fields in and below the photosphere and assumed charged particles traveled on orbits which would adiabatically preserve the magnetic flux through those orbits. As a result, charged particles are mirrored in the solar atmosphere. This greatly increases the solar albedo from what one might estimate neglecting the solar magnetic fields that just graze the Sun. The effect of mirroring on the total absorption rate is summarized by the coefficient A. Generally, the absorption rate of cosmic rays and, therefore, the signals we discuss, are proportional to the smaller of A and C_D (see eq. [2.26]).

The overall flux of γ-rays is sensitive to both the diffusion parameters and the details of the flux tube model. Our model leads to A and C_D which are comparable for the $E \sim 1$–10 GeV primaries responsible for most of the γ-flux. Thus, if we have underestimated the effects of either diffusion or absorption, our nominal predictions would have to be reduced. Both A and C_D would have to increase to give a significant increase in our results. Finally, it is possible that a fraction of cosmic rays are absorbed efficiently by the Sun, but not within flux tubes. In this case, albedo γ-rays would be suppressed. In fact, this is what we have assumed happens for primaries with energy $E > E_T$, but we argue that the threshold energy for confining particles to flux lines, E_T, is large enough that the main producers of photons are confined to field lines and do contribute to the albedo.

Similar comments hold for our predictions of solar albedo neutrons. The neutrino signal, on the other hand, is relatively insensitive to the details of our model. This is because the bulk of observable neutrinos have their origins in high-energy primaries, and the higher energy cosmic rays do not feel the effects of magnetic fields as severely.

Finally, although there is clearly some time before any of these potential signals is observed, it is possible that their observation would lead to a better understanding of other solar phenomena. For example, it is possible that correlations between an observed γ-ray flux and other solar variables could yield useful information on the structure of magnetic fields near the Sun. One might suppose that the origin ("footprint") of the interplanetary magnetic field on the Sun would influence where on the Sun most Galactic cosmic rays are absorbed, and this could yield an interesting correlation between the albedo γ-ray flux and the solar cycle. In addition, any γ-ray observation which showed details on the solar disk could yield a considerable amount of information on the magnetic fields in the corona and photospheric regions.

We are grateful to our colleagues at Bartol for much help concerning the propagation of cosmic rays in the heliosphere, especially John Bieber, Paul Evenson, Dermott Mullan, John Perko, and Bob Schaefer. We also thank Guarang Yodh and Fred Reines for stimulating conversations at the beginning of this project. This work was supported in part by NASA grants NAGW-1644 and NAGW-2076, and by the DOE under grant DE-AC02-78ER05007.

APPENDIX

Due to the importance of ^{4}He spallation as a neutron source, we felt it was necessary to develop a separate Monte Carlo to model neutron production. Our previous Monte Carlo's were concerned with electromagnetic showers (Stanev & Vankov 1989) or with lepton production (Gaisser & Stanev 1985). Neither required the inclusion of very soft hadronic processes associated with spallation, although they did include pion production.

The neutron production Monte Carlo includes six types of baryons: ^{4}He, ^{3}He, ^{3}H, ^{2}H, p, and n, which are considered either as target (at rest with respect to the Sun) or incident. Secondary baryons are considered as incident for subsequent collisions. The target consists of 10% ^{4}He and 90% protons by number. The mass 2 and 3 nuclei show up only as secondaries. Particles with $E < 100$ MeV per baryon are dropped—any neutrons they produce are unlikely to reach Earth's orbit before the neutrons decay.

We identify several types of interactions: inelastic collisions between two free nucleons, various spallation reactions involving

only soft momentum exchanges between nuclei, and interactions that combine both spallation and inelastic (i.e., pion production) processes. Elastic scattering of single nucleons is ignored since this process results in no change in nucleon flavor and the energy loss is small.

The cross sections for inelastic collisions are derived from $p - p$ and $n - p$ accelerator data. The inelastic interactions are treated in two ways. For incident kinetic energies below 1.5 GeV π production is treated as the result of Δ production and decay. At higher energies a multiparticle production model is used (Gaisser et al. 1988). The model includes a 28% probability for charge exchange for the incident nucleon.

Spallation may occur to the incident or target nuclei, or to both if the collision involves a compound incident nucleus and a ^{4}He target. Consider incident nucleus spallation first. The program begins by choosing the spallation channel using energy-dependent cross sections for spallation to different final states (e.g., $^4\mathrm{He} \rightarrow n^3\mathrm{He}$, ^2Hpn, etc.) given by Meyer (1972). Spallation of ^{4}He to $^2\mathrm{H}^2\mathrm{H}$ is rare due to the fragility of deuterium, and we neglect this channel. Each outgoing nucleon is given an energy equal to the average energy per nucleon of the incident nucleus, independent of the type of the spallation products. Next, we account for a small energy transfer between the incident nucleus and the target. One unbound spallation nucleon from the incident nucleus, is chosen randomly for a quasi-elastic energy transfer. The momentum transfer is sampled from a $d\sigma/dq \sim \exp(-q^2/q_0^2)$ distribution (Perkins 1987), where $q = 2k \sin(\theta/2)$ with k and θ the nucleon momentum and scattering angle in the center of mass frame, and $q_0^2 = 4$ GeV^2. The incident nucleon four-vector is then transformed to the solar rest frame, and the energy transfer to the target is calculated. If the energy transfer exceeds 100 MeV, the target proton is included in the cascade.

Next, consider spallation of target ^{4}He by an incident single nucleon. We determine the spallation products in the same fashion as for incident nucleus spallation; however, we slightly modify our treatment of the energy transfer. We determine the magnitude of the energy transfer using the same quasi-elastic procedure as above, except that the energy transfer is shared among all the fragmentation products using probability distributions for individual fragment energies taken from Meyer (1972), whereas for incident nucleus spallation the energy transfer was given to a single nucleon. In the incident spallation case, nearly all final state nucleons will pass our threshold test of 100 MeV, and so applying the energy transfer to a single nucleon rather than sharing it should make little difference to the final neutron spectrum. To implement a more careful scheme sharing the energy transfer would have required ad hoc assumptions about the angular distributions of the spallation products and did not seem justified. For target spallation, on the other hand, the energy transfers are comparable to our 100 MeV threshold, and so the effects of sharing the energy might conceivably make a substantial change to the distribution of neutrons. In this regard, the energy transfer to the target ^{4}He is small for low-energy incident nucleons, but rises to $\sim$360 MeV (90 MeV per nucleon) for incident energies above 2 GeV.

The last spallation case involves two compound nuclei. We do not have any experimental data on spallation probabilities in, for example, $^4\mathrm{He}^3\mathrm{H}$ collisions, so we treat each nuclear spallation as if it were caused by an individual nucleon ignoring the effects the spectator nucleons might have on the spallation probabilities. The energy transfer is calculated between a randomly selected unbound nucleon from the incident nucleus, but applied to all fragments of the target nucleus as described above.

Combined inelastic and spallation processes are handled in a fashion similar to pure spallation, except that the two participating nucleons are scattered inelastically instead of quasi-elastically. The inelastic scattering is treated as above. If the incident nucleus is compound, then the participating incident nucleon is given the energy per nucleon of its parent nucleus, while the target nucleon is at rest. No energy is transferred to spectator incident nucleons, but any target fragments are given energies determined using Meyer's probability distributions.

Total inelastic and spallation cross sections are not well known. There is little experimental data except Meyer's compilation, and the extensive tables for inelastic pp (Flaminio et al. 1984) and pn (Benary, Price, & Alexander 1970) interactions. The pp compilation includes several measurements of the $p - {}^4$He inelastic cross section. We have used the known cross sections to estimate the unknown ones. The inelastic cross sections for compound nuclei with proton targets are scaled down with atomic mass as

$$\sigma_{pA} = \sigma_{p4}\left(\frac{A}{4}\right)^{0.8}, \tag{A.1}$$

where the scaling is based on $E > 2$ GeV data taken from Flaminio et al. (1984). Below 2 GeV and down to the pion threshold, we scale the energy dependence of the cross sections to that measured in pp scattering. When both nuclei are compound (i.e., a ^{4}He target) we scale the inelastic cross sections to that for $^4\mathrm{He} - {}^4$He interactions, taken from much higher energies (Otterlund 1987). The scaling law for $A = 2$ and $A = 3$ nuclei on a helium target is

$$\sigma_{4A} = \sigma_{44}\left(\frac{A^{1/3} + 4^{1/3} - 1.12}{4^{1/3} + 4^{1/3} - 1.12}\right)^2, \tag{A.2}$$

derived by Westphall et al. (1979). We know of no comparable relations for spallation reactions, so we use equation (A.1) and (A.2) to scale the spallation cross sections to those known for ^{4}He reactions (Meyer 1972).

Having discussed the scattering processes included in the model we outline the overall structure of the Monte Carlo logic. For every incident nucleus both the spallation and interaction free path are sampled for both H and ^{4}He targets. Then the target and interaction type are chosen, after which the final state particle types and energies are determined. These particles are then treated as incident particles for the continuation of the cascade, except that particles with less than 100 MeV per nucleon are dropped since they will not contribute significantly to the observable neutron flux at Earth.

In addition to accounting for spallation products, the neutron Monte Carlo explicitly considers the trajectories of charged and uncharged particles in and near the Sun. Whenever a charged particle is produced, its trajectory is determined by adiabatically maintaining the flux through its orbit, until it either interacts again or escapes from the Sun. If a charged particle escapes, then it is

assumed that it will eventually reenter another photospheric flux tube with a new angle of incidence, until eventually it is absorbed. As discussed in § 2.3 the probability for a charged particle to escape the solar system, once it enters the Sun, is small for $E \lesssim 10$ GeV.

Neutrons, on the other hand, follow straight trajectories. Whenever a neutron escapes, it is propagated out to 1 AU, allowing for decay, where it is recorded along with its energy. Neutrons that interact within the Sun may produce secondary cascades separated spatially from the primary cascade. When this happens we compute a new set of charged particle trajectories based upon the magnetic fields at the new depth. In general, the new secondary cascade location will differ from the primary location horizontally as well as vertically. We use the same vertical field structure at the new horizontal coordinate, implicitly assuming that the mean free paths are shorter than the horizontal dimensions of a flux tube. This approximation is valid at the photosphere and gets better with depth. It is questionable for the $\sim 10\%$ of primary cascades initiated above the photosphere.

REFERENCES

Adams A., et al. 1990, Proposal to Construct the First Stage of the GRANDE Facility, GRANDE 90-005
Aguilar-Benitez, M., et al. 1990, Phys. Letters, 239B, 1 (Review of Particle Properties)
Baker, N., & Temesvary, S. 1966, Table of Convective Stellar Envelope Models, 2d ed., Institute for Space Studies (Goddard Space Flight Center: NASA)
Baldo Ceolin, M., ed. 1990, 2d Internat. Workshop on Neutrino Telescopes, Venice, Italy
Benary, O., Price, R., & Alexander, G. 1970, UCR-20000 NN (Univ. California, Riverside)
Casper, D. W. 1990, Experimental Neutrino Physics and Astrophysics with the IMB-3 Detector, Ph.D. thesis, Univ. Michigan
Chupp, E. L. 1987, ARA&A, 22, 359
Chupp, E. L., et al. 1987, ApJ, 318, 913
Dermer, C. D. 1986, A&A, 157, 223
DUMAND, II Proposal. 1988, Hawaii DUMAND Center Report HDC-2-88
Fichtel, C. E. 1989, Nucl. Phys. Proc. Suppl., 10B, 3 (Proc. Workshop on High Resolution Gamma Ray Astronomy, ed. D. Cline & E. Fenyves)
Fichtel, C. E., & Kniffen, D. A. 1984, ApJ, 134, 13
Fichtel, C. E., et al. 1977, ApJ, 217, L9
Fisk, L. A., Forman, M. A., & Axford, W. I. 1973, J. Geophys. Res., 78, 995
Flaminio, V., Moorhead, W. G., Morrison, D. R. O., & Rivoire, N. 1984, CERN-HERA Report 84-01
Frye, G. M., Jr., Dunphy, P. P., Chupp, E. L., & Evenson, P. 1988, Sol. Phys., 118, 321
Gaisser, T. K., & Grillo, A. 1987, Phys. Rev. D, 36, 2752
Gaisser, T. K., & Schaefer, R. 1991, in preparation
Gaisser, T. K., & Stanev, T. 1985, Phys. Rev. Lett., 54, 2265
Gaisser, T. K., Stanev, T., & Barr, G. 1988, Phys. Rev. D., 38, 85
Gelmini, G., Gondolo, P., & Roulet, E. 1991, Nucl. Phys. B, in press
Gleeson, L. J., & Axford, W. I. 1968, ApJ, 154, 1011
Hillas, A. M. 1984, ARA&A, 22, 425
Hudson, H. S. 1989, in Proc. Gamma Ray Observatory Workshop (Greenbelt: Goddard Space Flight Center), 4-351
Kamionkowski, M. 1990, Fermilab preprint Pub-90/181-A
Kanbach, G., et al. 1989, in Proc. Gamma Ray Observatory Workshop (Greenbelt: Goddard Space Flight Center), 2-1
Kuznik, B. (for the Frejus Collaboration). 1987, Orsay Preprint LAL-87-21
Lockwood, J. A. 1973, Space Sci. Rev., 14, 663
Lohmann, W., Kopp, R., & Voss, R. 1983, CERN Yellow Report 83-03
Losecco, J. M., et al. 1987, Phys. Letters, 188B, 388
Mayer-Hasselwander, H. A., et al. 1982, A&A, 105, 164
Meyer, J. P. 1972, A&AS, 7, 417
Murphy, R. J., Dermer, C. D., & Ramaty, R. 1987, ApJS, 63, 721
Nordlund, A. A., & Stein, R. F. 1990, in Solar and Stellar Granulation, ed. R. J. Rutten & G. Severino (Dordrecht: Kluwer), 453
Otterlund, I. 1987, Nucl. Phys. A, 461, 113c
Palmer, I. D. 1982, Rev. Geophys. Space Phys., 20, 335
Parker, E. N. 1958, ApJ, 128, 664
Perkins, D. H. 1987, Introduction to High Energy Physics (Menlo Park: Addison-Wesley)
Perko, J. 1987, A&A, 184, 119
Priest, R. E. 1982, Solar Magnetohydrodynamics (Dordrecht: Reidel)
Primack, J., Seckel, D., & Sadoulet, B. 1988, Ann. Rev. Nucl. Part. Sci., 38, 751
Protheroe, R. J. 1982, ApJ, 254, 391
Ramaty, R., Miller, J. A., Hua, X.-M., & Lingenfelter, R. E. 1990, ApJS, 73, 199
Sato, N., et al. 1990, KEK Preprint 90-166
Seckel, D. 1990, Trends in Astroparticle Physics, in press
Silk, J., Olive, K. A., & Srednicki, M. 1985, Phys. Rev. Lett., 55, 257
Spruit, H. C. 1981, The Sun as a Star, ed. S. Jordan (NASA SP-450) (Washington: GPO)
Stanev, T., & Vankov, H. P. 1989, ApJ, 343, 828
Stephens, S. A., & Golden, R. L. 1987, Space Sci. Rev., 46, 1
Vernazza, J. E., Avrett, E. H., & Loeser, R. 1973, ApJ, 184, 605
Volkova, L. V. 1980, Soviet. J. Nucl. Phys., 31, 784
Webber, W., & Potgieter, M. 1989, ApJ, 344, 779
Westphal, G. D., Wilson, L. W., Lindstrom, P. J., Crawford, H. J., Greiner, D. E., & Heckman, H. H. 1979, Phys. Rev. C, 7, 1309
Zirker, J. B. 1981, The Sun as a Star, ed. S. Jordan (NASA SP-450) (Washington: GPO)